International Journal of Modern Physics B
Vol. 20, Nos. 30 & 31 (2006) 5154–5163

World Scientific
www.worldscientific.com

QUANTUM MONTE CARLO STUDY OF OVERPRESSURIZED LIQUID ^{4}HE AT ZERO TEMPERATURE

LEANDRA VRANJEŠ MARKIĆ

Faculty of Natural Sciences, University of Split, N. Tesle 12, 21 000 Split, Croatia
Institut für Theoretische Physik, Johannes Kepler Universität, A 4040 Linz, Austria
leandra@pmfst.hr

JORDI BORONAT*, JOAQUIM CASULLERAS and CALUDIO CAZORLA

Departament de Física i Enginyeria Nuclear, CampusNord B4-B5,
Universitat Politècnica de Catalunya, E-08034. Barcelona. Spain
**jordi.boronai@upc.es*

We present a diffusion Monte Carlo simulation of metastable superfluid ^{4}He at zero temperature and pressures beyond freezing ($\sim$ 25 bar) up to 275 bar. The equation of state of liquid ^{4}He is extended to the overpressurized regime, where the pressure dependence of the static structure factor and the condensate fraction is obtained. Along this large pressure range, excited-state energy corresponding to the roton has been determined using the release-node technique. Our results show that both the roton energies and the condensate fraction decrease with increasing pressure but do not become zero. We compare our calculations to recent experimental data in overpressurized regime.

Keywords: ^{4}He; excitations; Monte Carlo.

1. Introduction

Fluids in metastable phases, both below the saturated vapor pressure and above the freezing point, present a research topic of fundamental interest for both experiment and theory.[1] The extreme purity of liquid helium at very low temperatures allows researchers to avoid nucleation on impurities and walls, and thus makes it the best suited system for the study of homogeneous nucleation, an intrinsic property of the liquid.

The negative pressure regime has been extensively studied by Caupin, Balibar and collaborators using an acoustic technique, in which high intensity ultrasound bursts are focused in bulk helium and the possible nucleation of bubbles or crystals is studied by shining laser light through the acoustic focal region.[2,3] In liquid ^{4}He they have measured a negative pressure only 0.2 bar above the spinodal point of -9.6 K predicted by microscopic theory.[4,5] By slightly modifying their experimental setup, so as to avoid nucleation on the walls, the same group has recently succeeded in pressurizing the small quantities of liquid ^{4}He up to 160 bar at temperatures 0.05 K $< T <$ 1 K.[6] This is the highest pressure ever realized in liquid metastable ^{4}He and

is much larger than the liquid-solid equilibrium pressure, which at $T = 0$ K is 25.3 bar. All along this large increase of the liquid pressure beyond the freezing point no solidification was observed. It is not clear if a limit exist to how far one can pressurize liquid helium. Namely, there is a significant difference in the nature of the two metastable phases. At negative pressure, there exists an end point (spinodal point) where the speed of sound becomes zero. Since at this point compressibility becomes infinite it is thermodynamically forbidden to cross it maintaining a homogeneous liquid phase. So, below that pressure the liquid brakes into droplets. Such type of an end point does not exist on the overpressurized side. However, as the excitation energy of rotons decreases with pressure (a fact well-known from the stable phase), Schneider and Enz[7] suggested that the pressurized phase has also an end point corresponding to the pressure where the excitation energy of the roton might vanish. On the other hand, Jackson *et al.*[8] and Halinen *et al.*,[9] find another instability that could cause the liquid-solid transition in ^{4}He which involves a soft mode having 6-fold symmetry in the two-body correlations.

It is also interesting to find out what the nature of metastable liquid ^{4}He at these high pressures is; superfluid or liquid. Recent experiments have shown that by immersing liquid ^{4}He in different porous media one can create metastable phases, at both negative pressures and pressures above the stable phase, that have a long enough lifetime to allow study by neutron scattering.[10,11] In this way information on the phonon-roton excitations has been obtained for negative pressures up to -5 bar[10] and overpressures up to ~40 bar.[11] The results of the latter experiment by Pearce *et al.*[11] show the roton excitation falling with pressure in the overpressurized regime, between 25 and 38.5 bar, while no roton is observed in the solid phase. At the liquid-solid transition, the roton energy is still finite, which means that ^{4}He is superfluid when it crystallizes. This result seems to be in disagreement with a recent experimental work by Yamamoto *et al.*[12] who reported superfluid transition temperature approaching $T_c = 0$ at a pressure $P \sim 35$ bar in a porous material, which implies the existence of a quantum phase transition from superfluid to normal liquid at zero temperature. It is possible that the differences observed in the two experiments are a consequence of the different pore diameters used (44 Å in Ref. 11 and 25 Å in Ref. 12), but additional work is needed to confirm this argument. In the direction of quantum phase transition, Nozières[13] has predicted recently that the condensate fraction could vanish at a certain pressure, and therefore a normal liquid before solidification would be possible.

Contrary to the negative pressure region where theoretical knowledge is rather complete,[1] the overpressurized liquid has remained nearly unexplored, especially at the level of microscopic treatment. Recently, we have applied diffusion Monte Carlo (DMC) method to the overpressurized phase up to $P \sim 275$ bar.[14,15] We considered it probably the best suited way to deal with this metastable regime because the physical phase of the system is controlled by the trial wave function used for importance sampling. Our results, in particular those for condensate fraction and the excitation energy of the roton, show that metastable helium remains superfluid all

along the large pressure increase from the solidification up to the highest pressures studied. In this paper, we will first present our calculations of the ground state and then proceed to excitations corresponding to the roton.

2. Ground State

The DMC method is nowadays a well-known tool in the of study quantum fluids and solids at zero temperature. For this reason we shall only give here the basic expressions. This fully microscopic approach solves stochastically the imaginary-time Schrödinger equation.

$$-\hbar\frac{\partial\Psi(\boldsymbol{R},t)}{\partial t} = (H - E_t)\Psi(\boldsymbol{R},t)\ , \tag{1}$$

where E_t is a constant acting as a reference energy, $\boldsymbol{R} \equiv (\boldsymbol{r}_1, \ldots, \boldsymbol{r}_N)$ is a *walker* in Monte Carlo terminology and the N-particle Hamiltonian is given by expression

$$H = -\frac{\hbar^2}{2m}\sum_{i=1}^{N}\boldsymbol{\nabla}_i^2 + \sum_{i<j}^{N}V(r_{ij})\ . \tag{2}$$

The He-He interaction $V(r)$ corresponds to the HFD-B(HE) Aziz potential.[18] The usual practice is to introduce the trial wave function $\psi(\boldsymbol{R})$ for importance sampling and to rewrite the Schrödinger equation in terms of $\Phi(\boldsymbol{R},t) = \Psi(\boldsymbol{R},t)\psi(\boldsymbol{R})$. In the limit $t \to \infty$ only the lowest energy eigenfunction, not orthogonal to $\psi(\boldsymbol{R})$, survives. For the ground state of bosonic system, such as liquid ^{4}He, the DMC gives exact results apart from the statistical errors.

The trial wave function for the simulation of the liquid in its ground state is of Jastrow type. As in the previous calculations in the stable domain,[16] we have used a model proposed by Reatto[17] which includes nearly optimal short and medium range two-body correlations

$$\psi(\mathbf{R}) = \prod_{i<j}\left(-\frac{1}{2}\left(\frac{b}{r_{ij}}\right)^5 - \frac{L}{2}exp\left[-\left(\frac{r_{ij}-\lambda}{\Lambda}\right)^2\right]\right), \tag{3}$$

This model has variational parameters L, λ, Λ and b, which were optimized in a variational Monte Carlo calculation.[14]

In order to compare our results with the behavior of solid ^{4}He, we have also carried out DMC simulations of the crystalline hcp phase. In this case, the trial wave function is given by a Nosanow-Jastrow model

$$\psi_{NJ}(\boldsymbol{R}) = \psi_J(\boldsymbol{R})\prod_{i}^{N}h(r_{iI}), \tag{4}$$

where $h(r)$ is a gaussian function linking every particle i to a fixed lattice point $\boldsymbol{r}_I$.

We have assumed periodic boundary conditions in all the simulations. Since the densities in this study are relatively large it has been necessary to carry out

a detailed analysis of the parameters influencing the simulation in order to eliminate possible bias. The most important check concerns residual size effects. This is achieved by summing proper tail corrections to the partial components of the energy (potential and kinetic) and by calculating the energies using different number of particles N. We have found this number increasing with density, from $N = 150$ near freezing to $N = 250$ at the highest density. In addition, the dependence on the mean population of walkers and the time step in the employed second-order algorithm[16] has also been carefully determined to eliminate any possible systematic error.

The complete equation of state, from the spinodal point up to the highest densities is plotted in Fig. 1. We have found that DMC energies are accurately param-

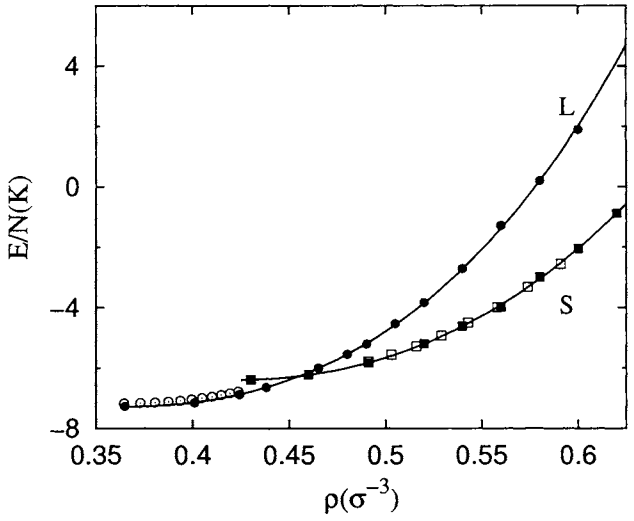

Fig. 1. Energy per particle of liquid ^{4}He from the equilibrium density up to the highest density calculated, 0.6 σ^{-3}, (solid circles). The solid line corresponds to the fit to the DMC energies using Eq. (5), and the open circles are experimental data in the stable regime from Ref. 19. DMC results for the solid phase are shown as solid squares and compared with experimental data from Ref. 20 (open squares). The error bars of our data are smaller than the size of the symbols.

eterized, from the spinodal point up to the highest densities in our calculation, by the analytical form[14]

$$e(\rho) = e_0 + e_1\,(\rho/\rho_c - 1)\,(1 - (\rho/\rho_c - 1)) + b_3(\rho/\rho_c - 1)^3 + b_4(\rho/\rho_c - 1)^4\ , \quad (5)$$

with $e = E/N$, and $\rho_c = 0.264\ \sigma^{-3}$ ($\sigma = 2.556$ Å) the spinodal density. The rest of parameters in Eq. (5) are $e_0 = -6.3884(40)$ K, $e_1 = -4.274(31)$ K, $b_3 = 1.532(12)$ K, and $b_4 = 1.433(24)$ K, the figures in parenthesis being the statistical errors.[14] Fig. 1 also shows DMC results for the energies of the solid phase, calculated using the Nosanow-Jastrow trial wave function and an hcp lattice. In all the density regime studied, the system is ***artificially*** maintained in a homogeneous liquid phase. The

comparison between the liquid and solid phase simulations shows clearly that DMC is effectively able to study the overpressurized liquid phase in spite of not being the ground-state (minimum energy) configuration, which obviously corresponds to the solid phase beyond the freezing point. This can be achieved by the DMC method because the physical phase is implicitly contained in the importance sampling trial wave function and it is not changed along the simulation. DMC should arrive at the *true* ground state (solid) in the limit of infinite simulation time. Since achievement of this limit requires breaking of symmetry imposed by the importance sampling wave function, it is not observed in the usual time schedules. In particular, in the course of our simulations we have observed no signal of freezing and therefore the results obtained correspond unambiguously to the metastable liquid phase.

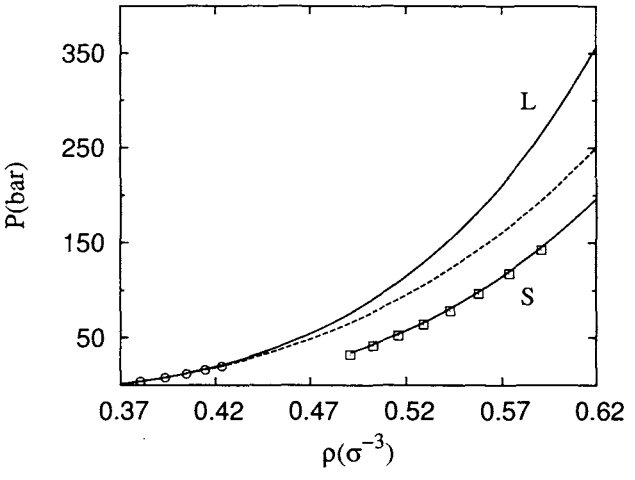

Fig. 2. Pressure as a function of the density. The solid lines stand for the DMC results obtained from the equations of state of the liquid and solid phases shown in Fig. 1. The dashed line is the extrapolation from experimental data;[6,21] the symbols correspond to experimental data for the liquid[19] and solid phases.[20]

Using the equation of state (5), we have obtained the pressure from its thermodynamic definition

$$P(\rho) = \rho^2(\partial e/\partial\rho). \tag{6}$$

The results, shown in Fig. 2, reproduce accurately the experimental data[19] of the pressure as the function of the density in the stable regime and predict a pressure $P \simeq 275$ bar at the highest density evaluated, $\rho = 0.6\ \sigma^{-3}$. They are compared in the same figure with the analytic form suggested in Ref. 6, adjusted to Abraham's experimental data.[21] Below the freezing point, both curves agree but they give significantly different values at higher densities; the difference amounts to $\sim$ 100 bar at $\rho = 0.6\ \sigma^{-3}$. As a matter of comparison, the pressure of the solid phase, derived from the DMC equation of state is also shown in Fig. 1. Similar discrepancies

between our results and the extrapolations of the experimental data from the stable region appear at high pressure results of the speed of sound and amount to almost 200 m/s at the highest density.[14]

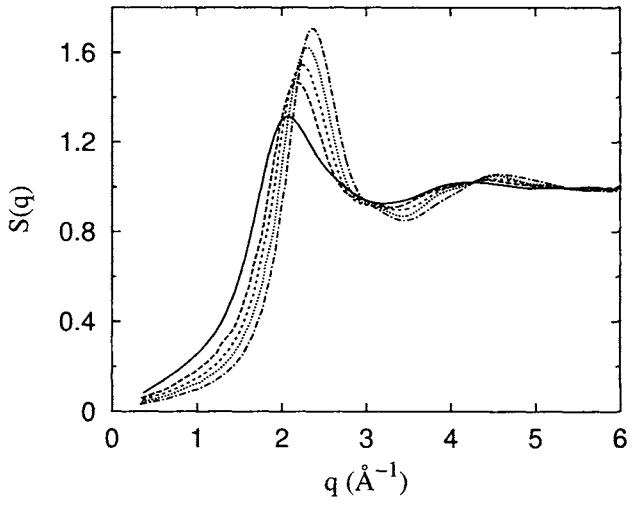

Fig. 3. Static structure function of the liquid phase for different densities. From bottom to top in the height of the main peak, the results correspond to densities 0.365, 0.438, 0.490, 0.540, and 0.6 σ^{-3}.

An important quantity in the study of quantum liquids is the static structure factor $S(q) = \langle \rho_q \rho_{-q} \rangle / N$, with $\rho_q = \sum_{i=1}^{N} e^{iq \cdot r_i}$. Our results are reported in Fig. 3, for densities ranging from the equilibrium up to the highest densities studied. The results show the expected behavior: when ρ increases, the strength of the main peak increases and moves to higher momenta in a monotonic way. At low momenta, the slope of $S(q)$ decreases with the density, following the limiting behavior $\lim_{q \to 0} S(q) = \hbar q/(2mc)$ driven by the speed of sound c. A characteristic feature of a solid phase is the presence of high-intensity peaks of the static structure function in the reciprocal lattice sites. Following the overpressurized liquid phase, we have not observed this feature which confirms the liquid nature of the system. According to Schneider and Enz, the instability of the liquid against the solid ought to be accompanied by the blowup of the main peak of $S(q)$.[7] Here, we see a rather slow growth of the main peak with pressure which indicates that the predicted instability is located much higher in pressure.

A characteristic signature of bulk superfluid ^4He is a finite value of its condensate fraction, i.e., the fraction of particles occupying the zero-momentum state. As usual in a homogeneous system, we have extracted the condensate fraction n_0 from the long range behavior of the one-body density matrix, $\lim_{r \to \infty} \rho(r) = n_0$. To this end,

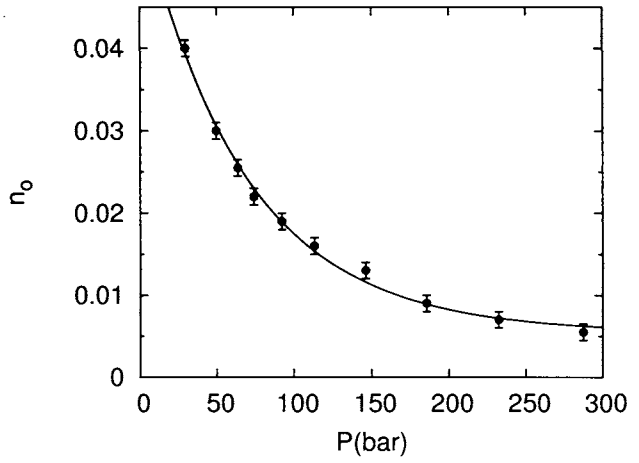

Fig. 4. Condensate fraction of liquid ^{4}He in the overpressurized regime. The line is an exponential fit to the DMC results.

$\rho(r)$ is sampled by means of the quotient

$$\left\langle \frac{\psi(\boldsymbol{r}_1,\ldots,\boldsymbol{r}_i+\boldsymbol{r},\ldots,\boldsymbol{r}_N)}{\psi(\boldsymbol{r}_1,\ldots,\boldsymbol{r}_i,\ldots,\boldsymbol{r}_N)} \right\rangle , \tag{7}$$

evaluated in the configuration space, over a set of random displacements $\boldsymbol{r}$ of particle i. The results obtained for n_0, from the melting pressure up to nearly 300 bar, are plotted in Fig. 4. The line on top of the data corresponds to an exponential fit which reproduces quite accurately our DMC results. As one can see in the figure, n_0 decreases quite fast until $P = 100$ bar and then the slope decreases, approaching a value $n_0 \simeq 0.005$ at the highest density. With the same procedure, we obtained[16] $n_0 = 0.084(1)$ at the equilibrium density $\rho_0 = 0.365\ \sigma^{-3}$, value which is compatible with PIMC estimations at low temperature[22] (0.069(10) at $T = 1.18$ K and 0.087(10) at $T = 1.54$ K). An exponential decay of n_0 with density up to pressures ≈ 80 bar was also obtained using the variational path integral method (VPI) in Ref. 23. VPI method, using a similar estimator as in PIMC, gives n_0=0.069(5) at ρ_0.

3. Excited State

It has been experimentally demonstrated that the energy of the roton excitations reduces with rising pressure.[11,24] The vanishing of the roton energy at some pressure has been proposed as the intrinsic instability limit of the liquid against a solid. This hypothesis led us to carry out a DMC released-node (RN) calculation of the roton energy beyond the freezing point. The same methodology was used in the past in a DMC calculation of the phonon-roton spectrum at equilibrium and freezing densities[26] arriving at an accurate description of the experimental data. The simulation of the roton is more involved than the simulation of the ground state because of the sign problem associated with the excited state wave function. As

a trial wave function for importance sampling we have taken an eigenstate of the total momentum operator which incorporates backflow correlations, as originally proposed by Feynman and Cohen,[25] $\psi_{BF}(\boldsymbol{R}) = \psi_e(\boldsymbol{R})\psi_J(\boldsymbol{R})$, where

$$\psi_e(\boldsymbol{R}) = \sum_{i=1}^{N} e^{i\boldsymbol{q}\cdot\tilde{\boldsymbol{r}}_i} \tag{8}$$

with $\tilde{\boldsymbol{r}}_i = \boldsymbol{r}_i + \sum_{j\neq i}^{N} \eta(r_{ij})\boldsymbol{r}_{ij}$, and $\eta(r) = \lambda \exp[-((r-r_b)/\omega_b)^2]$. In the DMC implementation of the program we have used a superposition of the states with momenta $\boldsymbol{q}$ and $-\boldsymbol{q}$ which are degenerate in energy. This enabled us to avoid working with a complex wave function. In this way the calculation of the excited state energy turned into a fermion-like problem since the resulting trial wave function is real but not positive everywhere.[26] In a first step, we have used the fixed-node (FN) approximation, which provides an upper bound to the roton energy. We have verified that the introduction of backflow correlations in the trial wave function produces results quite close to experimental data at the equilibrium density, especially near the roton minimum. The nodal constraint imposed by FN is removed, in a second step, by using the RN technique. In the RN approach, walkers are allowed to cross the nodal surface imposed by ψ and survive for a finite lifetime t. This is achieved by introducing the auxiliary guiding wave function $\psi_g(\mathbf{R})$, positively defined everywhere, which approaches the $|\psi(\mathbf{R})|$ away from the nodal surface and is non-zero in the nodes. The function $\psi_g(\mathbf{R}) = \psi_J(\mathbf{R})(\psi_e^2(\mathbf{R}) + a^2)^{1/2}$ achieves this goal for the proper choice of parameter a. The excited state energy is estimated through an exponential fit $E(t) = E_r + Ae^{-(t/\tau)}$, with t the released time. The uncertainty of this extrapolation is under control since in all cases the difference between considering the last calculated point in released time or E_r is of the same order as the statistical noise. The energy of the roton is then expressed as the difference between the excited and the ground state energy $\epsilon_r = E_r - E_0$. Since both the ground and the excited state energy have statistical errors, the resulting errors for the roton energy are quite large and difficult to reduce.

The results for the roton energy as a function of the pressure are shown in Fig. 5 and compared to experimental data obtained by neutron scattering experiments on superfluid ^{4}He in a porous media and up to 40 bar.[11] From 0 to 40 bar, the measured ϵ_r decreases linearly with the pressure and our data reproduces well this behavior. However, increasing the pressure we find that this slope is reduced. At the highest density studied the roton energy is still different from zero ($\epsilon_r = 2.8 \pm 1.2$ K at $\rho = 0.58\ \sigma^{-3}$). At each density, the number of particles has been adjusted to be as close to the roton momentum as possible. Due to the finite size of the simulation cell only discrete values of $\boldsymbol{q}$ are accessible , so corrections to the energy due to this fact are possible. However, we estimate them to be less than 0.5 K in all cases. In Fig. 6 we show the obtained values of the roton momentum and compare them with the measurements in the stable[24] and overpressurized regime.[11] Our results do not follow linear dependence with pressure, as the data in the stable liquid regime

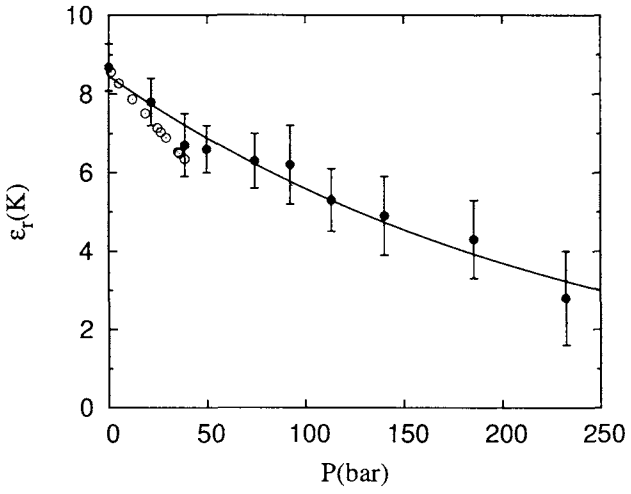

Fig. 5. Roton energy as a function of the pressure (solid circles). Open circles stand for experimental data from Ref. 11. The line is an exponential fit to the DMC data.

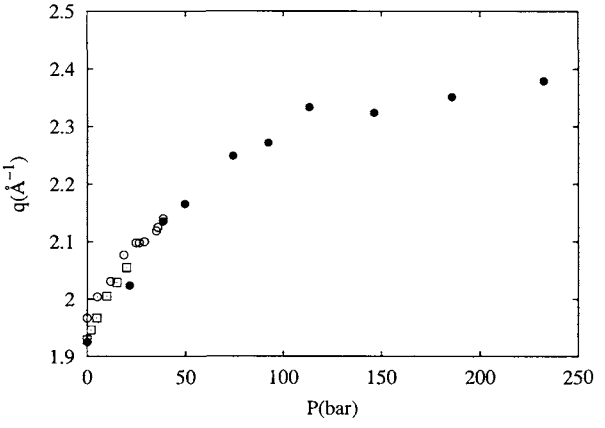

Fig. 6. Roton momentum as a function of the pressure (solid circles). Open circles stand for experimental data from Ref. 11 and open square for experimental data from Ref. 24.

might suggest.[24] As the pressure is increased, the slope of the roton momentum as a function of pressure decreases.

4. Conclusion

It has been shown that overpressurized metastable liquid ^{4}He can be studied with DMC method.[14,15] Along the pressure range from freezing to almost 300 bar, no signature of liquid/solid instability appeared. The finite value of condensate fraction and roton gap imply helium ^{4}He remained superfluid despite the fact that the

pressure increased more than 10 times. Static structure factor, condensate fraction and roton energy are however driven by the density (which increased less than 50% from freezing to maximum density studied) and not by the pressure. As can be seen in the Fig. 2, equal density increments in the stable and metastable regime produce clear differences in the pressure increase. This leads, in the density range studied, to an approximated exponential decrease with rising pressure of magnitudes like n_0 and ϵ_r.

Acknowledgments

We thank M. Barranco, F. Caupin, J. Navarro, and M. Saarela for useful discussions. Partial financial support from DGI (Spain) Grant No. BFM2002-00466 and Generalitat de Catalunya Grant No. 2001SGR-00222 is gratefully acknowledged. We acknowledge the support of Central Computing Services at the Johannes Kepler University in Linz, where part of the computations were performed.

References

1. *Liquids Under Negative Pressures*, edited by A. R. Imre *et al.* (Kluwer Ac. Publishers, Dordrecht, 2002).
2. F. Caupin and S. Balibar, *Phys. Rev.* **B64**, 064507 (2001).
3. S. Balibar, *J. Low Temp. Phys.* **129**, 363 (2002).
4. J. Boronat *et al.*, *Phys. Rev.* **B50**, 3427 (1994).
5. G. H. Bauer *et al.*, *Phys. Rev.* **B61**, 9055 (2000).
6. F. Werner, G. Baume, A. Hobeika, S. Nascimbene, C. Herrman, F. Caupin, and S. Balibar, *J. Low. Temp. Phys.* **136**, 93 (2004).
7. T. Schneider and C. P. Enz, *Phys. Rev. Lett.* **125**, 1186 (1971).
8. A. D. Jackson *et al.*, *Phys. Rev.* **B24**, 105 (1981).
9. J. Halinen *et al.*, *J. Low Temp. Phys.* **121**, 531 (2000).
10. F. Albergamo *et al.*, *Phys. Rev. Lett.* **92**, 235301 (2004).
11. J. V. Pearce, J. Bossy, H. Schober, H. R. Glyde, D. R. Daughton, and N. Mulders, *Phys. Rev. Lett.* **93**, 145303 (2004).
12. K. Yamamoto, H. Nakashima, Y. Shibayama, and K. Shirahama, *Phys. Rev. Lett.* **93**, 075302 (2004).
13. P. Nozières, *J. Low Temp. Phys.* **137**, 45 (2004).
14. L. Vranješ, J. Boronat, J. Casulleras, J. *Low Temp. Phys.* **138**, 43 (2005).
15. L. Vranješ, J. Boronat, J. Casulleras, C. Cazorla, *Phys. Rev. Lett.* **95**, 145302 (2005).
16. J. Boronat and J. Casulleras, *Phys. Rev.* **B49**, 8920 (1994).
17. L. Reatto, *Nucl. Phys.* **A328**, 253 (1979).
18. R. A. Aziz *et al.*, *Mol. Phys.* **61**, 1487 (1987).
19. R. De Bruyn Ouboter and C. N. Yang, *Physica* **B44**, 127 (1987).
20. D. O. Edwards and R. C. Pandorff, *Phys. Rev.* **140**, 816 (1965).
21. B. Abraham *et al.*, *Phys. Rev.* **A1**, 250 (1970).
22. D. M. Ceperley and E. L. Pollock, *Can. J. Phys.* **65**, 1416 (1987).
23. S. Moroni and M. Boninsegni, *J. Low Temp. Phys.* **136**, 129 (2004).
24. M. R. Gibbs *et al.*, *J. Phys.: Condens. Matter* **11**, 603 (1999).
25. R. P. Feynman and M. Cohen, *Phys. Rev.* **102**, 1189 (1956).
26. J. Boronat and J. Casulleras, *Europhys. Lett.* **38**, 291 (1997).